# Theoretical Analysis of Long Range Turbulent Transport in the Scrape-Off-Layer

Ph. Ghendrih 1), Y. Sarazin 1),
G. Attuel 1), S. Benkadda 2), P. Beyer 2), C. Clément 1), G. Falchetto 1),
C. Figarella 2), X. Garbet 1), V. Grandgirard 1), M. Ottaviani 1)

1) Association Euratom-CEA, DRFC/DSM/CEA CEA Cadarache,
13108 St-Paul-lez-Durance, France
2) UMR 6633 PIIM CNRS-Université de Provence, 13397 Marseille Cedex 20, France

e-mail contact of main author : ghendrih@drfc.cad.cea.fr

**Abstract.** Simulations of Scrape-Off Layer (SOL) turbulence with free energy content (flux driven) are characterized by profile relaxation and strong outward bursts of density. The ballistic propagation extends well beyond the e-folding length of the SOL. Turbulence stabilisation is achieved by biasing part of the limiter surface. The critical radial extent to achieve this stabilisation is derived. This effect governs the size of the biased ring required to insulate the wall from the long range bursts of matter. The same characteristic scale also governs the critical size of Langmuir probe tips. For probe tips in excess of this size, the flux tube to the probe is found to be decoupled from the background plasma.

## 1 Introduction

In the course of predicting the performance of a next step device, it is recognised that scaling the edge transport is rather uncertain. Since, the edge transport leads to severe constraints in the operating window of the device -such as the energy transfer to the divertor, the H-mode barrier formation, ELM relaxation and main chamber recycling- it appears crucial to improve the understanding of the turbulent transport in this region of the plasma. Furthermore, long range transport in the Scrape-Off Layer (SOL) has been reported in several experiments [1, 2]. These transport events do not appear to fit into the standard view of diffusive transport. Recent theoretical analysis of flux driven transport provide a qualitative understanding of these observations [3]. Theoretical investigation of cross-field transport in the SOL thus remains an important task both to assess theoretical models of turbulent transport and to increase confidence in the modelling effort in view of the operation of ITER-FEAT. Finally, the relatively easy measurements of SOL profiles and fluctuations provide a good test bed for theoretical models of turbulent transport, both core and edge.
The paper is organised as follows. In Section 2, the outstanding features of flux driven transport in the SOL as well as the model used for these investigations are presented. Electric current flowing in the SOL are found to determine the turbulent activity. Biasing then provides a means to insulate part of the limiter from the large particle flow due to the bursts of density. This effect is analysed in Section 3 and applied to both insulating the main chamber wall with a biased poloidal ring and analysing the interplay between SOL turbulence an Langmuir probe measurements.

## 2 Flux driven turbulence and ballistic transport

The model of SOL transport used in this work is a 2D fluid model based on the interchange instability in the SOL [4, 5]. The sheath boundary conditions introduce parallel loss terms, both to set the particle flux to the ion saturation current and to ensure a vanishing current flux. The problem is further simplified by considering constant temperatures with $T_i << T_e$. The system is then reduced to that of two fields, namely the density, $n = n_e/n_0$ where $n_0$ is a reference density, and the electric potential, $\phi = eU/T_e$ where U is the electric potential and e the electric charge.

$$\begin{aligned} \frac{\partial}{\partial t} n + [\phi, n] &= -\sigma\, n \exp\left(\Lambda - \phi\right) + D \nabla_\perp^2 n + S \\ g\ \partial_y Log(n) + \frac{\partial}{\partial t} \nabla_\perp^2 \phi + [\phi, \nabla_\perp^2 \phi] &= \sigma \left\{ 1 - \exp\left(\Lambda - \phi\right) \right\} + \nu \nabla_\perp^4 \phi \end{aligned} \tag{1}$$

Time and space are normalised respectively to $1/\Omega_i$ the ion cyclotron frequency and to $\rho_s$, the hybrid Larmor radius. The Poisson brackets are defined by $[f, g] = \partial_x f \partial_y g - \partial_y f \partial_x g$ where $x$ and $y$ are the normalised radius $x = (r - a)/\rho_s$ and poloidal coordinate, $y = a\theta/\rho_s$. The parallel loss term is set by the floating potential $\Lambda$ and the characteristic time of parallel transport $\sigma = \rho_s/L_{//}$ [6]. The two diffusion coefficients (normalised to the Bohm value), D for the particles and $\nu$ for the vorticity, govern the damping of the small scales. The curvature drive is proportional to $g \sim \rho_s/R$ where R is the major radius of the torus. Finally, S is the source term that maintains the system out of equilibrium. Numerical simulations are carried out on a $256 \times 256$ grid, the mesh size being $\rho_s$. With the parameters used in the present runs, this corresponds to a 0.08 m $\times$0.08 m box size. Flux driven transport, namely transport at given outflux rather than given gradients, is characterised by the occurrence of intermittent transport [3]. When examining the Probability Distribution Function (PDF) of the flux, one finds that both negative flux (influx) and positive flux occur. In the vicinity of zero flux, the PDF is found to be near a gaussian distribution. A long tail dominates at large positive flux. Using the standard deviation of the gaussian fit, one finds that 44 % of the flux is due to events at more than 4 standard deviations.

This "microscopic" description of transport thus departs very strongly from the random phase approximation that leads to a diffusive description of transport. However, when analysing the average density profile in the SOL, $< n >_{turb.}$ on *FIG. 1*, one finds an exponential fall-off that can also be analysed in terms of an effective diffusion coefficient. The e-folding length of the profile is of $50\rho_s$, hence in the 0.01 m range. For the sake of comparison the SOL profile with no turbulent transport $< n >_{col.}$ is also plotted on *FIG. 1*. The e-folding length is much shorter $\sim 7\rho_s$. The effective diffusion coefficient due to the turbulent transport is then 55 times larger than the collisional diffusion term introduced in the code.

In contrast to the standard SOL width, captured by the average profile, one finds that the long range ballistic events, called avalanches or fronts, extend over a significant fraction of the box, typically larger than $150\rho_s$. The gradients at the front location are very sharp with a characteristic scale that can be smaller than $5\rho_s$. Such gradients can also be observed on *FIG. 1* on the density profile $n_{turb.}$ (at a given time and poloidal location). The shape of the propagating front is not aligned along the $x$ or $y$ axis but exhibits "wiggles". As a consequence, the radial profile drawn at a given poloidal location will intersect the front at several distinct radial locations. This density profile thus exhibits very strong density gradients both positive (opposite to the average gradient) and negative.

The Mach number of these radially propagating fronts is of the order of $M_\perp \sim 0.1$. The radial range of the bursts $\Delta_\perp$ is then governed by the balance between the parallel

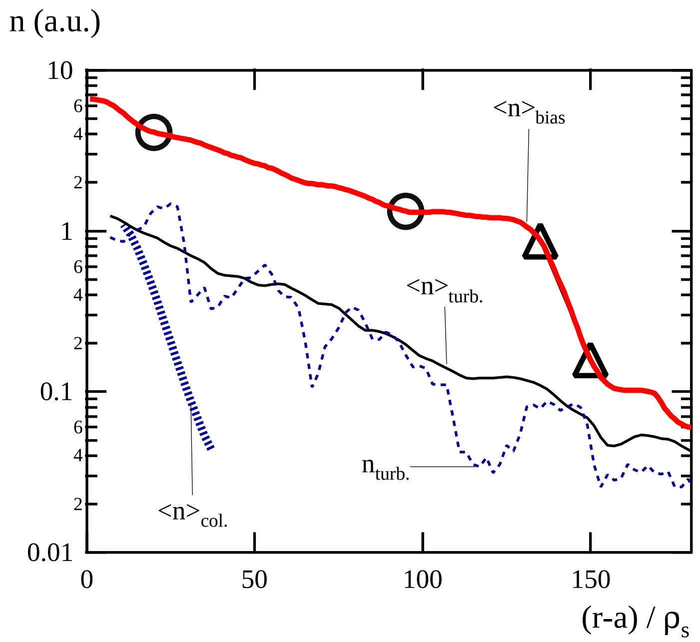


*FIG. 1 : SOL profiles, mean and local profiles, lower traces, with biasing, upper trace.*

transport along the connection length $L_{//}$ and the cross-field transport, one finds :

$$\frac{\Delta_\perp}{L_{//}} \sim \frac{M_\perp}{M_{//}} \tag{2}$$

Given $M_{//} \sim 1$ at the sheath [6], $\Delta_\perp$ would reach 0.1 $L_{//}$. (with the present runs, $\Delta_\perp \sim 0.1$ m is achieved). It would then be impossible to withdraw sufficiently the wall components of the main chamber to prevent plasma-wall interaction. However, one finds that the ballistic propagation of the density fronts is impeded by poloidal flows, the so-called zonal flows [7, 8]. This effect governs the "wiggles" discussed above. Enhancing this effect might provide a control of long range transport in the SOL.

## 3 Turbulence stabilisation with biasing

When analysing the vorticity equation, one finds that two currents control the evolution of the electric potential, the curvature driven current, proportional to the poloidal density gradient, and the parallel current to and out of the sheath. At lowest order in the electric potential fluctuations, the parallel current is $\pi/2$ phase shifted with respect to the radial particle flux. In the non-linear regime, this relationship still holds approximately. Driving a parallel current should then modify the cross-field transport. Implication of this effect is investigated both to design a means to insulate the main chamber of the tokamak from the long range bursts of matter and to analyse the interplay between Langmuir probe measurements and the SOL turbulence.
The sheath conductivity $\sigma$, see Eq. 1, governs the strong coupling of the plasma potential $\phi$ to the wall potential $V_{bias} + \Lambda$. Let $L_y$ be the scale of the poloidal gradient of the density field. The balance between parallel and curvature currents then yields.

$$\frac{g}{L_y \sigma} \sim 1 - \exp(\Lambda + V_{bias} - \phi) \tag{3}$$

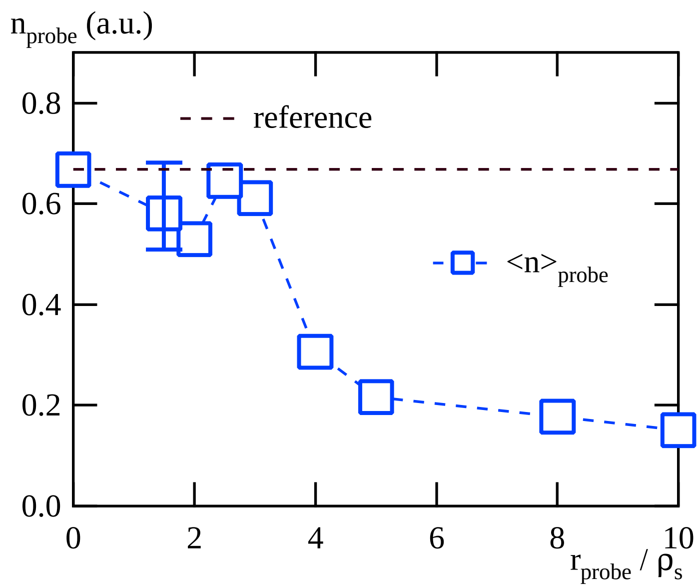


*FIG. 2 : Change in the measured density versus the size of the probe tip. The error bars indicate the magnitude of the fluctuations during the averaging*

If $g/(L_y\sigma)$ is small, $\sigma \rightarrow \infty$, the plasma potential is prescribed by the wall potential, $\phi \sim \Lambda + V_{bias} \pm |\frac{g}{L_y\sigma}|$. In particular the shear of the electric field and higher derivatives of this field will be controlled by $V_{bias}$. Conversely, for large values of the LHS of Eq. 3, a larger departure from the wall potential will be achieved. Other physics will then contribute, such as the Reynold stress related to the vorticity convection in Eq. 1.
Let us consider the interplay between Langmuir probe measurements and the SOL turbulence. The probe tip is modelled by a prescribed plasma biasing $V_{bias}$ over a limited extent of space. For convenience a gaussian shape with equal poloidal and radial extent is used. In a series of simulations, the probe radius $r_{probe}$ is scanned from 10 to $1.5\rho_s$. The value of the density at the probe tip is compared to the reference value with no biasisng (case $r_{probe} = 0$), see *FIG. 2*.
The mean density measurement is recovered when the probe tip is smaller than $3\rho_s$. This value is smaller than the characteristic scale of the collisional diffusion $(D\sigma)^{1/2} \sim 7\rho_s$. It is then set by the constraint given in Eq. 3 where $L_y$ is governed by the scale of variation of $V_{bias}$ namely the probe size. With the values chosen in the simulations, one finds a critical size of the probe tip $g/\sigma \sim 2.5\rho_s$ in agreement with the simulations. When the probe tip is smaller than this critical value, cross-field currents feed into the biased region and the plasma potential is not modified by the probe biasing. When the probe exceeds the critical value, the plasma potential remains close to the biasing potential. This induces a vortex at the probe tip, with a strong shear of electric drift. A linear analysis shows that the stabilising effect of the third derivative of the plasma potential is large enough to quench the turbulence at the probe location. The flux tube is then insulated from the neighbouring plasma and the density at the probe tip is governed by the balance between parallel and collisional transport. This leads to a large density decay at the measurement point.
The previous analysis provides the basis to determine the means to insulate the main chamber wall of the tokamak from plasma-wall interaction. A biased ring is used to stabilise the SOL turbulence and prevent the density burst from reaching the wall. Such

a scheme is realistic insofar that low plasma temperature and low density in the distant SOL will reduce the current flowing to the biased ring and thus the required power to sustain the biasing potential. The parameters of the biasing ring have been set according to the results of the Langmuir probe simulations, namely a gaussian shape radially with an extent of $10\rho_s$ (typically 5 mm) with no poloidal dependence. The biasing ring generates a transport barrier in the outer SOL, see *FIG. 1.* Towards the separatrix, the e-folding length is unaffected (between the circles) while it is reduced to the collisional value at the biasing ring (between the triangles). A test of the strength of this insulating barrier has been achieved by generating large avalanches with a very localised density source. In the simulations, none of these large burst have crossed the transport barrier. Further investigation of this concept is required, especially regarding the possible occurrence of barrier relaxation mode (reported in transport barrier simulations [9]).

## 4 Discussion and conclusion

Turbulent transport investigation without prescribing the mean gradient or the energy content of the system is characterised by strong intermittency. Profile relaxations and steepening of the gradients lead to front like dynamics. These bursts characterise the long range transport in the SOL. They extend well beyond the exponential e-folding length of the mean SOL profile.

Biasing of wall components can modify locally the turbulent transport. This is deleterious to the Langmuir probe measurement for probe tips exceeding a critical size. In the calculation of this critical size, good agreement is found between the predicted value and that observed in the simulations. Biasing can be beneficial if one aims at insulating the tokamak main chambers from the density bursts. Robust transport barriers can be achieved with relatively narrow poloidal rings of biased wall components.

### Acknowledgements

Part of this work was done during the "Festival de Théorie", Self-Organization and Transport in Electromagnetic Turbulence, Aix-en-Provence, France, July 2001.

### References

[1] RUDAKOV, D.L., et al., Plasma Phys. Control. Fusion, **44** (2002) 717.

[2] LABOMBARD, B. et al., Nucl. Fusion, **40** (2000) 2041.

[3] SARAZIN, Y., GHENDRIH, Ph., Phys. of Plasmas, **5** (1998) 4214.

[4] NEDOSPASOV, A.V., Sov. J. Plasma Phys., **15** (1989) 659.

[5] GARBET, X., et al., Nucl. Fusion, **31** (1991) 967.

[6] STANGEBY, P.C., McCRACKEN, M.C., Nucl. Fusion, **30** (1990) 1225.

[7] DIAMOND, P.H., et al., in *Proceedings of the 17th IAEA Fusion Energy Conference, Yokohama, 1998* (IAEA, Vienna, Austria, 1999), Vol. 4, p. 1421.

[8] SARAZIN, Y., et al., *Theoretical understanding of turbulent transport in the SOL*, to be published in J. Nuclear Mater.

[9] BEYER, P., et al., *Electrostatic Turbulence and Transport with Stochastic Magnetic Field Lines*, this conference, contribution IAEA-CN-TH/4-2.